Glass formation in simple ionic systems via constant pressure molecular dynamics

Prashant N. Kumta, Pierre A. Deymier, and Subhash H. Risbud
Department of Materials Science and Engineering, University of Arizona, Tucson, Arizona 85721

(Received 21 December 1988; accepted 6 March 1989)

The utility of constant pressure molecular dynamics (MD) in studies of glass formation is demonstrated by choosing NaCl and $ZnCl_2$ as examples of MX and MX_2 salts. Rigid ion pair potentials have been used to model the two salts. Results of these simulations are in good agreement with general glass formation principles. The effect of the interatomic potential on the glass transition and the cooling rate on glass formation in both the salts is reported. The parameter characterizing the inertia of the borders of the MD simulation cell has a strong influence on the glass transition temperature.

I. INTRODUCTION

The molecular dynamics (MD) method is currently one of the most powerful tools for deriving the macroscopic and microscopic properties of assemblies of classical particles using realistic interatomic potentials. MD consists of solving the classical equations of motion of an assembly of particles. To date, much of the research in the field of dynamical computer modeling has employed the standard method of MD in the microcanonical or canonical ensemble. With its ability to provide a full account of configurational time evolution, MD has been extensively utilized to study phase transitions. Early atomistic computer simulations of glass formation in simple monoatomic systems such as hard spheres or Lennard-Jones systems are well documented[1-3]. Attention has also been given to real glass forming systems.

Early studies of BeF_2 glasses have demonstrated the high degree of realism one could attain in a computer simulation.[4,5] Calculations of SiO_2 glass with purely ionic interactions have produced radial distribution functions very similar to that of vitreous silica[6]. Following these successes, molecular dynamics simulation technique has been more recently applied to the study of the structure of binary ZrF_4–BaF_2 glasses.[7-13] The results of these latter studies are sometimes contradictory and satisfactory comparisons with experimental data are not at all at hand.

It is important at this stage to state some of the limiting factors in achieving accurate computer model of ionic glasses. The difficulties in realizing a precise model of ionic glasses are twofold. Lack of realism may originate from the potentials used to describe the interactions between the ions. For bonds with a high degree of ionicity, spherical two-body potentials and in particular exponentially decaying repulsions are reasonable approximations. However, caution is needed in applying potentials fitted to perfect lattice data to disturbed configurations, as, for example, liquids or glasses.[14] In the case of bonds with a dominant degree of covalency, the use of spherical two-body potentials is no longer justified even though tetrahedral coordination in SiO_2 has been shown not to depend on the covalent character of the Si–O bond.[6]

The second reason for divergence between simulations and experiments lies in the molecular dynamics algorithm itself. The condition of constant volume puts some restrictions on the relaxation processes the simulated system may undergo. Constant volume simulations will constrain the system to explore a limited region in amorphous phase space yielding configurations outside the neighborhood of the natural free-energy minimum as some fluctuations may not be allowed. In the study of phase transitions such as glass formation in which volume fluctuations are critical, isobaric MD is to be preferred over constant volume MD.

The effect of system size and time scale are of considerable importance. In the case of simple monoatomic fluid, the system size affects the rate of structural relaxation in the metastable system[15] and nucleation may be a serious problem in small systems ($N < 100$).[16] No systematic studies of the size effect on properties of ionic systems are available but trends similar to the monoatomic fluids can be expected. The consequence on glass formation of quenching liquid with extremely high cooling rates has been discussed at length by Woodcock *et al.*[6] In view of the extreme character of cooling rate in computer studies, one has to be careful in taking the frozen-in state obtained in simulations as a model for experimentally obtained glass although better agreement between computer simulated glasses and real glasses can be expected in tetrahedral network type glasses.

Computer simulations of glass formation in microcrystals of MX compounds (KCl) containing 512 ions have been reported.[17] In their study, Amini and Hockney have employed an inverse power interionic potential. A change upon cooling in the value of the specific heat at approximately 1/3 of the melting temperature (T_f) is taken as signalling a glass transition. A slight increase in the unlike ions coordination number from 4.0 to 4.6 is observed on cooling from the liquid to the glass state. Woodcock *et al.*[6] have seen similar results in a triply periodic infinite KCl system containing 216 ions. The short range interaction was modeled with an exponentially decaying repulsion as well as Van der Waals attraction terms. In this latter study, isobaric vitrification was obtained by interpolation from a series of molecular dynamics simulations at constant volume. Discontinuities in the first derivatives of the temperature dependence of the volume and enthalpy at $1/3T_f$ were taken as signs of a glass transition. In addition, the diffusion coefficient extrapolates to zero at this same temperature. Woodcock *et al.* report a splitting of the

 0021-9606/89/127384-11$02.10

first peak for the like ions partial radial distribution functions for the glass.

It would seem from these results that KCl has a well-defined minimum in amorphous phase space; and that a glass transition temperature at approximately $1/3T_f$ can be expected in this system. However in view of the very different conditions used in both studies, we believe that similarities between these two pieces of work may be fortuitous and generalization to other MX systems or other computer simulation conditions will have to be taken with great care. Indeed, simulations of NaCl under constant pressure indicate that a transition similar to laboratory glass transitions is taking place at approximately 2/3 of the melting point. Partial crystallization in small computer models of NaCl is found to be a limiting factor in obtaining good computer glasses.

The structure of molten $ZnCl_2$ has long been considered by molten salt chemist as one which is at large different from other halide salts due to the very high viscosity of the melt and its very high tendency to supercool to a glassy state. The glass transition temperature of $ZnCl_2$ is 388 K which is approximately 2/3 of the melting point, $T_m = 590$ K. The earliest MD simulation results on $ZnCl_2$ glasses were reported by Woodcock *et al.*[6] They performed simulations at constant volume using a Born–Mayer–Huggins-type pair potential. Their simulations predicted a Zn–Zn correlation distance which was in excess of more than 23% of the experimental value. Further improvements by Woodcock *et al.*[6] claiming reduction in this error have been referred to in the paper by Desa *et al.*,[18] however, no information on the parameters used in the potential have been reported. Based on calculation of diffusivity, they assigned 650 K as their "computer glass transition temperature." The cause for the disagreement between the calculated properties of the liquid state of this model and experimental values for energy, coordination numbers and partial radial distribution function have been recently attributed to the large degree of covalency of the Zn–Cl bond.[19]

Attempts to improve the model have been reported by,[19] Inoue *et al.*,[20] and recently by Hirao *et al.*[21] These authors have tried to simulate the liquid structure by incorporating changes in the Zn^{2+} ion radius and in the charges of the Zn and Cl species; however, apart from subtle improvements, the structure by and large still seemed far from the experimentally determined liquid structure.[18,22]. Ballone *et al.*[23] qualitatively examined the relationships between the interionic forces and the structure of $ZnCl_2$. In their study they stressed the need to incorporate angle-dependent interionic forces for more realistic computer modelling of molten $ZnCl_2$.

Based on the work by Ballone *et al.*[23] we have recently developed and reported a rigid ion model which gives a satisfactory description of the structure of $ZnCl_2$ in the liquid state.[24] This model, succeeds in bringing the Zn–Zn distance to 3.8 Å in agreement with experiment. Evaluation of coordination numbers suggest that the Zn^{2+} ions are predominantly tetrahedrally coordinated with a Zn–Cl–Zn bond angle of 111.2°. Combination of some fivefold and sixfold coordination for the Zn^{2+} ions are also seen in this model.

This paper presents an attempt to shed light on glass formation in ionic materials. A realistic constant temperature-constant pressure molecular dynamics algorithm has been used to investigate the formation of "glass-like frozen states" upon cooling for NaCl and $ZnCl_2$ as examples of MX and MX_2 salts. NaCl has been chosen because of its highly ionic character and poor glass forming ability, while $ZnCl_2$ can be obtained in the glassy state by using normal laboratory procedures and is known to form tetrahedral network glasses.

Rigid ion pair potentials have been used to model the two salts. The condition of the simulation as well as the character of the pair potentials are shown to play an important role on the glass forming ability and on the structure of the frozen state. The effect of the cooling rate on the computer simulations is reported and is shown to concur with generally accepted glass formation principles.

The results of the present work are discussed in three sections. Section II contains a brief description of the constant stress molecular dynamics formalism for systems of particle interacting through long-range Coulombic interactions. In Sec. III the results of the computations on metastable and glassy states of NaCl is presented. Finally Sec. IV contains results of simulations of $ZnCl_2$. The general principles and conclusions drawn from this study are reported in Sec. V.

II. METHOD AND MODEL

We have applied an extension of the constant stress molecular dynamics formalism of Parrinello and Rahman [PR][25] to the simulation of assemblies of particles interacting through long range Coulombic potentials.[26] This formalism allows for volume and shape variations of systems with periodic boundary conditions. The addition of these degrees of freedom are essential to the study of phenomena, such as phase transitions, in which volume fluctuations play a decisive role.[27]

The simulation of an assembly of ions involves the summation of the Coulombic energy potential and forces between all pairs. The long-range nature of these interactions yields very slowly converging series. The Ewald summation method[28] is incorporated into the MD algorithm to accelerate the convergence.

Most simulations in this study have been performed with the following set of conditions for the Ewald summation; $\eta = 5.6/L_{\max}$, the real space summations and reciprocal space summations have been truncated at $r_c = 1/2\, L_{\min}$ and $k^2 \leqslant 25 \times 4\pi^2$, respectively. $L_{\max}$ and $L_{\min}$ are the longest and shortest edges of the simulation cell. The contribution of the reciprocal space energy, force and internal stress to the total potential energy, force and internal stress matrix is within the noise level for these quantities. Thus no attempt was made to improve the convergence of the series in the reciprocal space.

In the PR MD formalism the edges of the simulation cell are described by three dynamically varying vectors. An arbitrary mass W which can be visualized as the mass of the boundaries of the simulation cell is assigned to each individual vector. Average properties of equilibrated systems calculated along the trajectories generated with the PR equations

of motion are independent of the mass of the borders while dynamical properties may not be.[29] The study of glass formation upon cooling of the melt is a highly nonequilibrium process and one can expect the results to vary with the parameter W. The effect of the parameter W will be particularly significant in the simulation of small systems. The increase of the period of oscillation of the volume fluctuations with W results in higher viscosity of the melt and larger relaxation times. Furthermore, the amplitude of the volume fluctuations decreases as W increases reducing the field of exploration for energy minima in the amorphous phase space. In order to extract valuable results from molecular dynamics simulations under constant pressure conditions, a realistic choice for W must be made. Andersen suggested that one may choose W based on matching experimental recovery time of the system from the imbalance between an external and the internal stresses.[30] Based on the above discussions a reasonable value of 5 was assumed for the parameter W in most of the simulations in the present study.

The PR equations of motion generate trajectories in the isoenthalpic-isostress ensemble. The isothermal condition was implemented with a momentum scaling procedure.[31] The constant pressure MD method deviates by an order N^{-1} from the constant enthalpy-constant pressure ensemble.[30] The momentum scaling method deviates from the canonical distribution[32] by an order $N^{-1/2}$. Phase space exploration by small systems using the above algorithm is, therefore, expected to differ from that of real systems. More realistic sampling of phase space can be realized with more refined constant temperature procedures[33] or simulation of significantly larger systems.

The pair potentials employed are Born–Mayer–Huggins type potentials:

$$\phi_{ij}(r) = Z_i Z_j e^2/4\pi\epsilon_0 r_{ij} + B_{ij} e^{(\sigma_{ij} - r_{ij})/\rho} - C_{ij}/r_{ij}^6, \quad i,j = +,-,$$

where r_{ij} is the distance between ions i and j, Z_i is the ionic charge and C_{ij} is a coefficient in the short range van der Waals attraction. The exponentially decaying repulsive term is composed of σ the sum of ionic radii, b_{ij} which is a hardness parameter and ρ which is a constant. The parameters used in the above equation were obtained from the model developed by Sangster *et al.*[34] in the case of NaCl. In the study of $ZnCl_2$ the parameters for the short range interaction were generated by us in the model referred to as KDR model.[24]

In generating a satisfactory set of parameters we have retained the hardness parameter of Woodcock *et al.*[6] We have also kept the same ρ reported by Gardner and Heyes [19] except for the Zn^{2+} interactions[24] in order to reduce the Coulomb repulsion between the Zn^{2+} cations. In view of the qualitative analysis by Ballone *et al.*[23] we reasoned that a modification of the Woodcock potential, with main emphasis on reduction of the strong Coulomb repulsion between the Zn–Zn ions, would result in successfully simulating the experimental liquid structure by MD. Based on the analysis of Woodcock and Ballone, the Coulomb repulsion between the Zn–Zn ions was reduced by introducing a van der Waals attraction component to the short range Zn–Zn interaction. A proper combination of the repulsion and attraction components results in effectively bringing the Zn–Zn correlation distance closer to the Cl–Cl distance as observed experimentally [22]

III. MX GLASSES

In this section we present results of computations on crystalline, liquid, metastable liquid and glassy states of NaCl. The short-range interactions are modelled by the exponentially decaying repulsive terms and van der Waals attractive terms of Sangster *et al.*[34] The system containing 216 ions has been simulated under a constant hydrostatic pressure of one atmosphere with an integration time step of 3.215×10^{-15} s. The mass of the boundaries of the simulation cell. W, has been chosen arbitrarily to be 5. Time averages have been calculated over the last 350 and 500 steps in the simulations lasting 400 and 600 steps, respectively. After heating the NaCl crystal up to the melting temperature, the system is completely randomized at 3000 K, then cooled to 1600 K and finally equilibrated at 1300 K. The liquid resulting from this treatment is used as starting configuration in four heat treatment paths as illustrated in Fig. 1.

In path one, the liquid is quenched at an infinite rate and the system equilibrated at room temperature for a period of 1200 time steps. Path two, three, and four correspond to a succession of step processes in which a change in temperature is imposed instantaneously followed by a constant-temperature anneal. Despite the fact that the system does reestablish an equilibrium state during the intermediate steps of path two, the annealing time is shorter than the time necessary to calculate satisfactory time averages; thus, averages of thermodynamic properties are not reported. Path two, three and four represent integrated cooling rates of $1.90\times10^{+14}$ K/s, $0.87\times10^{+14}$ K/s, and $0.58\times10^{+14}$ K/s, respectively System three has been subsequently reheated up to 1000 K. Longer simulations have been run at 800 K and 900 K for better equilibrations.

Variation of volume as a function of temperature is shown in Fig. 2. The enthalpy also shows a similar behavior. Very good agreement is noticed between experimental data

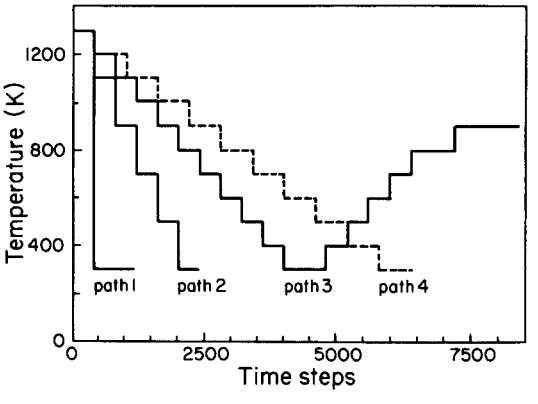

FIG. 1. Cooling and heat treatment paths followed in the simulations for NaCl. Each time step represents 0.32×10^{-14} s. Cooling rates for the various paths are Path 1: rapid quench; Path 2: 1.90×10^{14} K/s; Path 3: 0.87×10^{14} K/s; and Path 4: 0.58×10^{14} K/s.

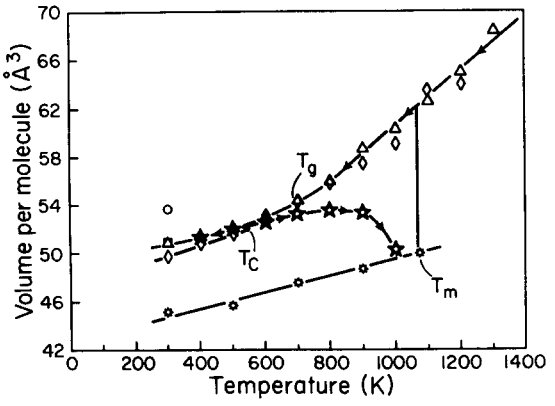

FIG. 2. Variation of cell volume per molecule as a function of temperature: ⊘, crystalline NaCl; ○, path 1; □, path 2; △, path 3; ◇, path 4; *, data for heat treatment of NaCl glass.

and calculated volumes of the crystalline and molten NaCl. The difference in volume between the liquid and crystalline state of 7.5 ± 0.05 cm^3/mol at the melting temperature is in excellent accord with experimental values. A latent heat of fusion of 33.2 ± 3 kJ/mol is computed. This energy compares reasonably well with the experimental heat of fusion of 28.0 ± 0.6 kJ/mol. A discontinuity in the derivatives of the volume–temperature and enthalpy–temperature plots in the temperature interval [700–800 K] is observed for path 3. This change taking place at approximately 2/3 of the melting point is characteristic of an experimental glass transition. The change in heat capacity from 79.8 J/K mol for the supercooled liquid to 59.0 J/K mol for the glass phase (C_p (liq)/C_p(glass) = 1.35) is characteristic of discontinuities for ionic glasses.[35] Despite the difference in cooling rates of path 2 and 3, both produce room-temperature glasses with identical volume and enthalpies. A twofold increase in quenching rate does not alter the volume of the frozen state in any significant manner. This result is inferred to the extreme magnitude of the cooling rates we employed. Though, the density of the glass prepared with an infinitely rapid quench is approximately 5% lower than the slowly cooled glasses. Path 1 is a succession of two stages; an infinitely rapid cooling at constant volume followed by an isothermal–isobaric relaxation period. The isochor cooling produces a frozen liquid which subsequently relaxes by ionic movement during the second step of the path. This result implies that the room temperature diffusivity vanish at a volume of $V_0 = 32.3$ cm^3/mol (see Fig.2). This suggests a first-approximation linear relationship between diffusivity and volume analogous to the "free volume" equation for diffusivity proposed by Hildebrand,[36] namely $D = A(V - V_0)/V_0$ where A is a constant. Assuming a constant V_0 and using the linear relation: V_{liq}(cm^3/mol) $= 0.013\,808 \times T$(K) $+ 22.70$, fitted to the calculated equilibrium volumes of the liquid; we obtain a temperature of 696 K at which the diffusivity vanishes. This latter temperature conforms well with the glass transition temperature observed during cooling path 3, suggesting that the break in the volume–temperature and enthalpy–temperature plots is related to a vanishing diffusivity.

The slowest cooling path no. 4 produces a volume–temperature plot similar to path no. 3 down to 600 K. Again a discontinuity in heat capacity and thermal expansion is observed at approximately 700 K. However, a discontinuity in volume is reported between 500 and 600 K indicating the onset of a first-order phase transition such as crystallization.

The structure of the glasses obtained with the cooling paths nos. 1, 2, and 3 are described by the partial radial pair correlation functions as well as distributions of local coordination of chlorine ions around sodium ions shown in Fig. 3. The like ions and unlike ions radial distribution functions of the NaCl liquid agree qualitatively with experimental functions of the melt[37] as well as calculated functions.[38] There is some evidence of a shoulder in $g_{+\,+}$ at 5.0 Å. The coordina-

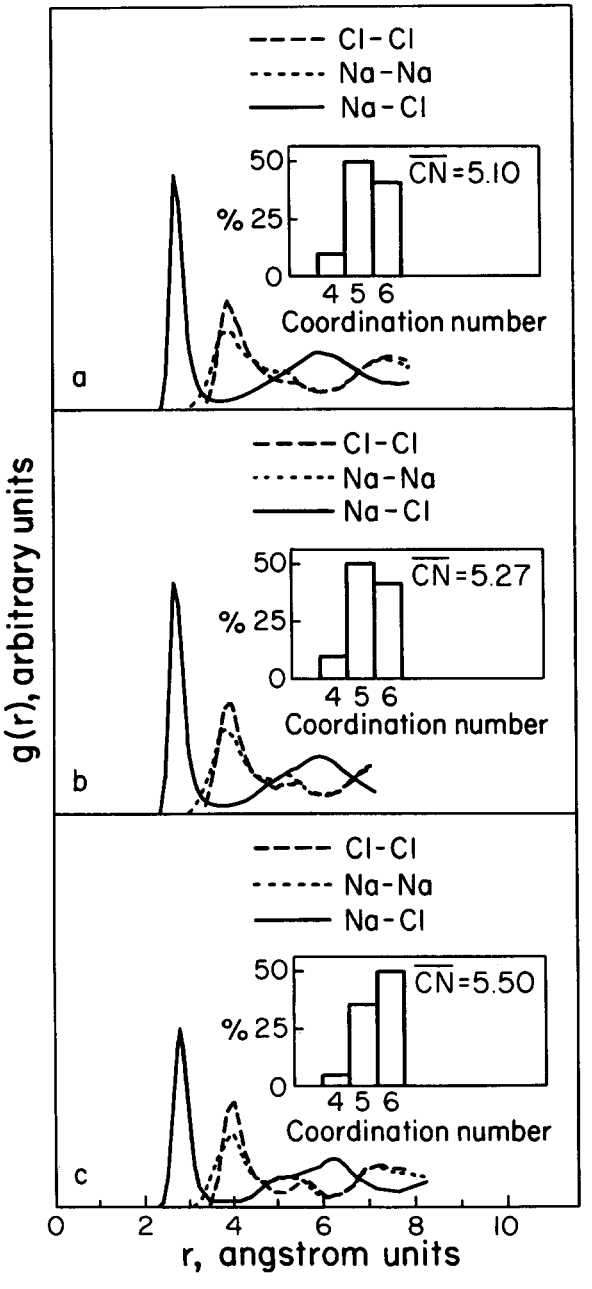

FIG. 3. Radial distribution function for the NaCl glasses (a) path 1, (b) path 2, and (c) path 3. Bar graphs in the inset show the unlike ion distribution of coordination number.

tion of Cl^- ions around Na^+ ions is 4.3 $\pm$ 0.2 at the highest temperature studied and increases to 4.9 $\pm$ 0.2 near the melting temperature. The glasses produced in cooling paths 1, 2, and 3, namely glasses 1, 2, and 3 differ structurally. There is very little difference between the pair distribution functions of glass 1 and the melt. One notices a wider shoulder in g_{++} and the initiation of a splitting of the first peak for the g_{--} distribution function. As the cooling rate decreases, a splitting of the first peak of the g_{++} function and sharper second peaks of the g_{--} function are observed. The position of the second peak of the g_{--} functions varies from 5.3 to 5.4 and 5.6 Å as the cooling rate decreases from path 1 to path 2 and path 3. We notice that these distances are 2 times the $+ -$ interionic distances.

Associated with this splitting is an increase in average local coordination. The coordination number of Cl^- about Na^+ increases from 5.1 to 5.3 and 5.5. This change in average coordination number results from a redistribution of ions with coordination 4 and 5 to a coordination 6. The splitting of the like ion distribution functions and the shift of local ion arrangement toward octahedral coordination appears gradually as the liquid is cooled. These tendencies are, however, less pronounced as the liquid is quenched more rapidly.

The splitting of the first peak of the like ion radial distribution functions is connected with the splitting of the second nearest-neighbor peak often observed for monoatomic amorphous close packing of spheres.[39,40] In MX ionic systems, the longer of the two preferred lengths corresponds to collinear arrangements of M–X–M or X–M–X triplets and the shorter to the distance of closest approach of a second X or M across an intervening pair of M or X constituting the basic polyhedron. A like–unlike ion distance of 2.83 Å (sum of the ionic radii) gives 4.00, 4.62, and 4.9 Å as distances of closest approach of like ions for square and octahedral, tetrahedral, triangular, and pentagonal coordinations, respectively. The length of aligned M–X–M or X–M–X triplets is twice the M–X distance in the case of an octahedron, that is 5.66 Å. Therefore, the shoulder observed in the like ion distribution functions of the liquid and glasses is correlated to the five fold coordinated ions; while, the second peak in the like ion distribution functions are associated to octahedral coordination. Indeed, the unlike ion distribution function of glass 3 exhibits secondary peaks at 4.9 Å and 6.3 Å which are characteristic distances of face and edge sharing octahedra.

A coordination number of 5.5 is calculated at 600 K during cooling path no. 4. Signs of edge and face sharing octahedra can be seen in the partial radial distribution functions. The change in coordination is gradual from 1300 to 600 K, however, a sudden increase in coordination to 5.7 is taking place at 500 K. At this latter temperature the partial radial distribution functions are characteristic of a phase with a high degree of crystallinity.

We believe that these results support the picture of a partially crystallized glass. The degree of crystallization or the amount of octahedrally coordinated ions is directly linked to the rate of cooling. Slow cooling rates produce large amounts of octahedra. Above some critical fraction of six fold coordinated ions, the packing of the polyhedra requires that the octahedra share edges and faces yielding secondary peaks in the unlike ion radial distribution function. We estimate this critical fraction of octahedral coordination at approximately 50%, that is an average coordination of 5.5. Thus, the cooling rate of path no. 3 represents a critical rate above which the degree of crystallization does not alter significantly the structure of the frozen state.

In order to study full crystallization of the computer glass, we reheated gradually glass no. 3 up to 1000 K. Longer simulations at temperatures above 700 K are needed for satisfactorily averaging properties. The volume–temperature plot corresponding to this heating treatment is reported in Fig. 2. At 600 K, the volume and enthalpy of the reheated glass start to depart from the values obtained during cooling. A sharp drop in the properties of the heated system toward the crystal properties begins after 800 K. The average coordination number increases from 5.5 at room temperature to 5.7 at 900 K. However, this increase is not gradual; no significant change in coordination number is observed up to 800 K. The partial radial distribution functions show a peak at 5.7 Å for the like ion functions and pronounced peaks at 5.2 and 6.5 Å for g_{+-}. At 1000 K, the system is entirely crystallized as indicated by a chlorine coordination around each sodium ion of 6. At this temperature, the radial distribution functions are characteristic of a NaCl crystal. The excess volume and enthalpy of the crystallized glass are due to defects which may have resulted from the artificial perio dicity introduced by the periodic boundary condition. It is interesting to note that crystallization starts at approximately 800 K at which the volume of the reheated glass approach the volume V_0 at which diffusion controlled relaxation may take place.

Questions arise regarding the size dependence of crystallization. In view of the results of Hsu and Rahman on monoatomic systems,[16] nucleation is a serious possibility in small systems ($N = 108$ atoms) simulated under periodic boundary conditions. Although crystallization upon cooling in a large Lennard–Jones (LJ) system ($N = 864$) has been reported.[41] This LJ system was simulated under constant temperature-constant pressure conditions. In that study, the cooling rate was found to be a determining factor in the formation of a glass or a crystal. The LJ system was crystallizing only when the cooling rate was below some critical value. In order to verify the possibility of a size dependence, we have simulated a small NaCl system containing 64 ions. Satisfactory convergence of the real space and reciprocal space series is attained with the condition: $\eta = 4/L_{\max}$, $R_c = 1.8L_{\min}$, and $k^2 < 9 \times 4\pi^2$. These conditions, however, introduce a strong artificial coupling between the simulation cell and its periodic images. Two cooling rates have been tested; an infinitely fast quench and a slow step process of 100 K per 600 time steps. The structure and properties of the crystalline and liquid phase of the small system agree well with the structure and properties of the larger one. Due to the small size of the system, the radial distribution functions extend to 6 Å, providing only limited structural informations. The infinitely rapid quench produces an amorphous phase. However, upon slow cooling the small system crystallizes readily at an undercooling of 274 K. These results are

consistent with the behavior of the larger system, although the latter crystallizes at a larger undercooling of 574 K. Simulations of NaCl systems significantly larger than in our study ($N > 500$) would shed more light on the size dependence of crystallization upon cooling. We have not been able to conduct such investigation because of computer limitations.

IV. MX_2 GLASSES

In this section we present results of computations on metastable liquid and glassy states of $ZnCl_2$. In contrast to MX salts such as NaCl, $ZnCl_2$ can be made into a glass very easily using conventional glass forming techniques. Two different sets of pair potentials were used in the present study, the first is a slightly modified version of the potential used by Woodcock *et al.* referred to hereafter as "modified WAC potential." The other one is a fundamental revision of the same potential namely the KDR potential.[24] Both potentials were used to simulate a system containing 324 ions (216 anions and 108 cations). Both systems were simulated under a constant hydrostatic pressure of one atmosphere. The integration time step is 0.65×10^{-14} s. Glass formation and supercooling using both models has been studied with a fully equilibrated liquid as the starting phase. The effect of the mass of the boundaries of the simulation cell on the ability to form a glass has been also investigated.

A. The modified WAC model

All simulations using this model were performed with $W = 5$. The liquid state was obtained by heating the $ZnCl_2$ crystal to 1200 K followed by an equilibration period lasting 7000 integration steps. The resultant liquid is comprised essentially of tetrahedrally coordinated polyhedra. The distribution of the unlike ion coordination shows 68% fourfold coordination, 25% fivefold coordination with sixfold coordination constituting only 7%. The partial radial distribution functions give values of 2.2, 3.55, and 4.2 Å as the first neighbor distances for Zn–Cl, Cl–Cl and Zn–Zn, respectively. The distance $r_{ZnZn} \sim 2(r_{ZnCl})$ indicates a linear linkage of the Zn–Cl–Zn triplet. This linear arrangement is also confirmed by the secondary peaks at 5.3 and 7.3 Å for the g_{+-} and g_{++} radial distribution functions.

The major difference between the modified WAC potential and the original WAC potential lies in the Zn–Zn distance of 4.2 Å as opposed to 4.7 Å while the experimentally observed distance is at 3.8 Å. This improvement resulted from the introduction of a van der Waals attraction term to the cation–cation potential. The modified WAC potential yields a value of 60.78 cm^3/mol for the equilibrium volume at $T = 1200$ K which is in excellent agreement with the experimental value of 61 cm^3/mol. The total energy, on the other hand, is still far from the experimental value (9% larger), nevertheless representing an improvement over the energy obtained with the WAC potential which was in excess of 17%.

$ZnCl_2$ "glasses" were prepared by cooling the the equilibrium liquid along two paths. In path 1, the liquid is quenched to 900 K and held for 6000 time steps, it is then subsequently quenched in a sequence of steps of 100 K. At every temperature, the system is then annealed for a period of 1000 time integration steps with time averages calculated during the last 800 time steps. This procedure results in an integrated cooling rate of 1.9×10^{13} K/s. Path 2 consisted of essentially freezing the liquid at 200 K and then equilibrating the system for a period of 1000 time steps. Along path 1 the volume and enthalpy vary linearly with temperature and no discontinuity in the first derivatives with respect to temperature is noticeable. The variation in the volume V, enthalpy H, and energy E, with temperature are given in the form

$$V(\mathrm{cm^3/mol}) = 5.74 \times 10^{-3} T(\mathrm{K}) + 54.376,$$

$$H(\mathrm{kJ/mol}) = 0.1058 T(\mathrm{K}) - 2440.15,$$

$$E(\mathrm{kJ/mol}) = 0.063 T(\mathrm{K}) - 2440.92.$$

The abscence of change in expansion coefficient and heat capacity suggest no perceptible glass transition, in agreement with the behavior of tetrahedrally coordinated network glasses wherein relaxation arrests occur primarily by steric restrictions. The average coordination number for the Zn–Cl ions does not show any significant change as the liquid is cooled. However, the distribution of the unlike ion coordinations of the glass at 200 K indicates a slight increase in the pentahedral coordination to 28% and a corresponding decrease in the octahedral coordination to 4%. The glass produced during path 1 retains the tetrahedral network nature of the liquid.

Freezing the liquid to room temperature (path 2) does not alter the structure of the glass in any appreciable manner. The coordination numbers for this glass do not indicate any significant difference with the glass obtained via path 1. Moreover, the equilibrium volume of this latter glass is, within statistical error equal to the volume of the glass obtained in path 1. This observation is again in agreement with the network nature of the system.

B. KDR Model

The KDR potential has been shown to give a realistic description of the $ZnCl_2$ liquid state.[24] The liquid consists of tetrahedra sharing vertices with a Zn–Cl–Zn triplet angle of 111.2°. The first nearest-neighbor distances for Zn–Cl, Zn–Zn, and Cl–Cl pairs are 2.3, 3.8 and 3.6 Å, respectively.

The liquid at 1200 K, however, comprises of not only 53% fourfold coordination but also of 31% fivefold and 16% sixfold coordination.

The equilibrium liquid at 1200 K used as starting point in the cooling processes has been obtained with a procedure identical to the modified WAC potential. It was observed that a 10-fold increase in the mass of the borders reduces the volume fluctuations of this liquid from 15% to 0.25% of the average volume. Glass formation has therefore been studied with particular relevance to the role played by the mass of the borders of the simulation cell. Two different values were used for the mass of the borders, in one case a value of 50 and in the other a combination of 50 and 5 was used. The results of these simulations will be reported as two different cases.

1. Effect of large mass of the borders of simulation cell on glass formation

Glass formation in this case has been studied by cooling the liquid along two different cooling paths. Path 1 similar to

the modified WAC liquid consists of cooling the liquid to 900 K and then to 700 K. Simulations at each of these temperatures were conducted for 6000 time steps. Subsequently, the liquid is cooled at intervals of 100 K followed by an annealing period lasting for 1000 steps. Time averages were calculated over the last 5000 steps for the long simulation and over the last 800 steps for the short one. Path 2 represents an infinite cooling condition. The liquid state is frozen instantaneously at 200 K and annealed for 6000 time steps. Equilibrium properties are calculated over the last 4000 steps. The variation of thermodynamic properties such as volume and enthalpy with temperature has been studied. The temperature dependence of the volume is illustrated in Fig. 4. Both volume and enthalpy exhibit a prominent break in their respective first derivatives at a temperature of 600 K approximately. This discontinuity is characteristic of a glass transition with a ratio of $C_p(\text{liq})/C_p(\text{glass}) = 1.2$. We tentatively call the arrest temperature a glass transition temperature.

Two distinct contributions to the variation in the coordination numbers above and below the glass transition temperature are reported. The partial radial distribution functions and distribution of coordination numbers at 700 and 300 K are collected in Fig. 5. The unlike and like ion coordinations of the liquid increases upon cooling from 1200 K to 700 K. A loss of 7% and 9% of fourfold and fivefold coordination, respectively, to the sixfold coordination occurs. The increase in the number of octahedra results in the appearance of new correlation distances in the partial radial distribution functions. The unlike ion pair distribution function shows two additional peaks at 4.5 and 7.9 Å corresponding to second and third closest distance of approach for unlike ions in a configuration of tetrahedra sharing corners with octahedra. Similar evolution of peaks are seen for in the partial radial distribution function for the like ion pair of Zn–Zn at 6.6 and 5.7 Å. These peaks are also a consequence of an increase in the sixfold coordinated linkages. On further cooling below the glass transition temperature the fourfold coordination decreases by another 3.7% transforming to the sixfold state. There is an onset of split in the peak for the radial distribution function g_{++} at 4.2 Å at 600 K. The split becomes very prominent at 300 K. However, there is no evidence of any split in the Cl–Cl pair radial distribution function suggesting that the Cl–Cl bond does not undergo any significant changes during cooling. The split observed in the peaks for the radial distribution function g_{++} is attributed to the increase in the sixfold coordination. In order to fit the emerging octahedra into the structure it is necessary to distort them. The distorted octahedra have an unlike ion shortest distance of approach of 2.9 Å which is larger than the characteristic distance of 2.3 Å. The linkage of distorted octahedra through their edges results in a Zn–Zn distance of 4.2 Å.

Structure of slow cooled glass and rapidly quenched glass: Cumulative radial distribution function (RDF) plots for the glass at 200 K obtained by path 1 and the rapidly quenched glass obtained by path 2 are superimposed in Fig. 6. The structure of both glasses are very similar and compare very well with the experimental plot obtained by Desa *et al.*[18] for vitreous $ZnCl_2$ shown in the inset. Though the RDF of the slow cooled and rapidly quenched glasses are very similar, there is considerable difference in the distribution of co-

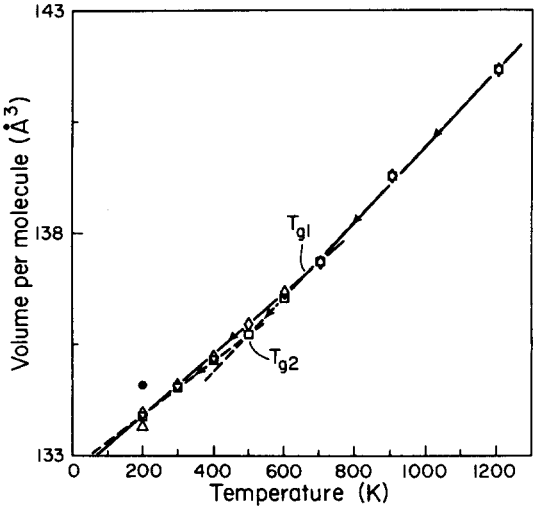

FIG. 4. Variation of cell volume per molecule as a function of temperature. ◇ represents variation during path 1 and ⊗ represents the data for rapid quench using W = 50. □ represents the variation during cooling path 1 and △ represents the corresponding data for rapid quench using W = 5 below $T = 700$ K. Path 1 in both cases corresponds to in integrated cooling rate of 9.05×10^{12} K/s.

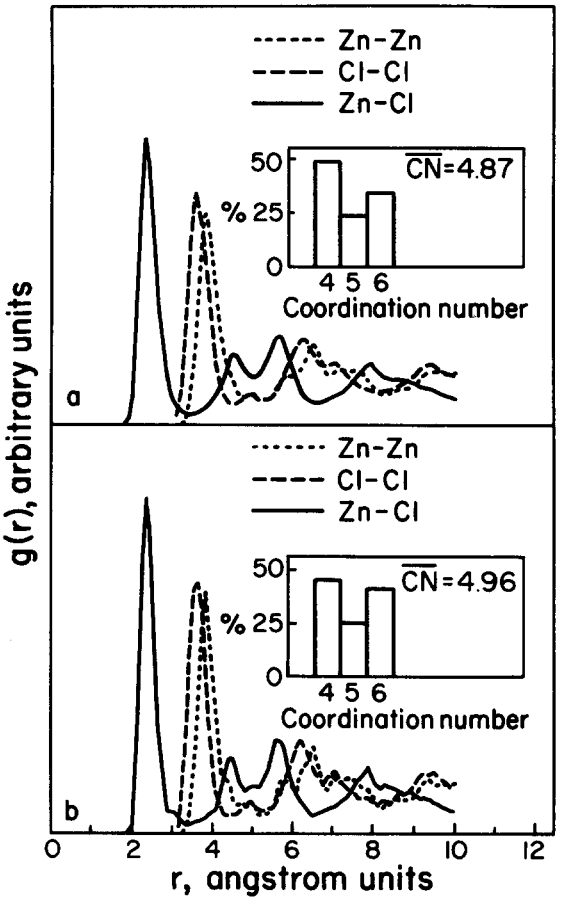

FIG. 5. Partial radial distribution function for liquid and glassy $ZnCl_2$ at (a) 700 and (b) 300 K, respectively, along path 1 with W = 50. The inset represents the distribution of unlike ion coordination number.

ordination numbers for the unlike ion pair. The distribution of coordination numbers for the rapidly quenched glass and the slow cooled glass is also reported in Fig. 6. The rapidly cooled glass retains about 5.6% more fourfold coordination as compared to the slow cooled glass. It also retains a smaller percentage (3.7%) of fivefold coordination. Slow cooling allows for more diffusion processes to operate resulting into more fivefold and sixfold coordinations. Evidence for the arrest of diffusional relaxation is also found in the average values for the equilibrium volume vs temperature graph (see Fig.4). The volume of the rapidly cooled glass is higher than that of the slow cooled one. This behavior is similar to that of an MX system. However, contrary to NaCl the volume is lower than the volume of the liquid at T_g suggesting that the volume does not obey the Hildebrand equation for free volume as seen in the case of NaCl. In the case of $ZnCl_2$, the nonobeyance of this equation could be hypothesised to be due to a nonlinear relationship of volume and diffusivity as steric relaxation is also expected to play an important role in densification upon cooling. In the rapid quench lasting 6000 time steps, the first 200 steps is the time frame during which a major portion of the diffusional and steric relaxation occurs. The volume drops by 8.2% during this interval. Beyond the first 200 time steps, we find that no further steric relaxation takes place resulting in a negligible volume fluctuation of only 0.03% in the last 4000 time steps of the simulation. Thus, the resultant glass configuration retains a large fragment of the four fold coordination from the liquid.

2. Effect of smaller mass of borders on glass formation

The effect of decreasing the mass of the borders was studied by using a combination of two different values for the parameter W during the process of cooling. The liquid structure was subjected to two cooling paths identical to those described in case 1. Two values were used for the parameter W during the course of the slow cooling schedule. The mass of the borders was set to 50 in simulation above 700 K. All simulations at 700 K and below were performed with W being assigned a value of 5.

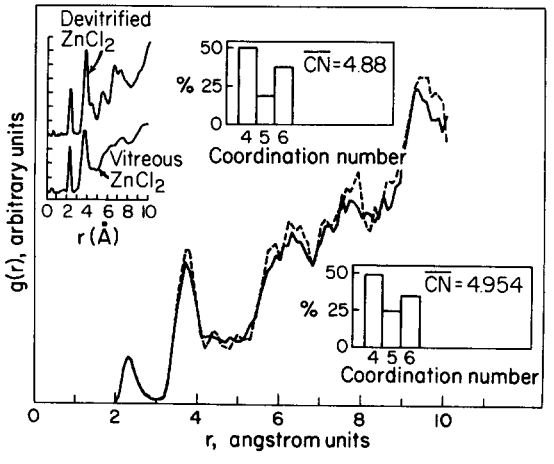

FIG. 6. Cumulative radial distribution function for $ZnCl_2$ glass at 200 K with W = 50. Solid line represents the distribution for rapidly quenched glass while the dashed line represents the distribution for slow cooled glass. The insets refer to the cumulative radial distribution function obtained experimentally (Ref. 18) and the unlike ion distribution of coordination numbers. $\overline{CN}$ of 4.954 and 4.88 refer to the average coordination numbers for the glass obtained along paths 1 and 2, respectively.

Effect of the cooling rate on the thermodynamic variables, namely, volume and enthalpy was again studied. Effect of reduction in the values for W is clearly reflected in the volume–temperature plot (see Fig. 4). The plot shows a prominent discontinuity in the first derivative of the volume with respect to temperature at 500 K which is 100° below the arrest temperature obtained in case 1 and approximately 100° above the experimentally observed glass transition. The ratio of heat capacity for the liquid and glass, $C_p(\text{liq})/C_p(\text{glass})$ is 1.2 as in case 1. We conclude that the parameter W affects the mobility of the ions and hence the fluidity of the melt resulting in lower glass transition temperature, the ratio of heat capacities across T_g remaining constant.

Effect of cooling rate on structure of the glass: The structure of the slow cooled glass exhibits identical features similar to those of the glass discussed in case 1. Increase in the sixfold coordination is again observed. This increase is, however, much more prominent than it was in the earlier case. At 700 K, the distribution of unlike ion coordination calculations indicate 42% fourfold, 26% fivefold and 32% sixfold coordination resulting in an average coordination of 4.91. The fourfold coordination decreases by 11.1%, the fivefold coordination decreases by 5.6% with reference to the liquid. Thus in contrast to case 1, reduction in W causes for a larger transfer of fourfold coordinated Zn^{2+} to sixfold coordinated Zn^{2+}. However, as the liquid is cooled to, and below the T_g of 500 K the fivefold coordination shows a larger percentage decrease in comparison to four fold coordination.

This results in an overall increase of about 26% in the sixfold coordination as opposed to 21% in case 1 for the glass at room temperature.

The radial distribution function for the system at each of the temperatures shows essentially the same features as in case 1 including the split in the peaks for the partial distribution functions g_{+-} and g_{++} at 2.9 and 4.3 Å, respectively.

Structure of slow cooled and rapidly cooled glasses: As in case 1 calculation of the distribution of coordination numbers for unlike ions reveals 35.2% fourfold coordination, 19.4% fivefold coordination, and 45.4% sixfold coordination in the case of the glass obtained by slow cooling at 200 K whereas, the rapidly quenched glass exhibits a distribution of coordination numbers of 48.15% fourfold coordination, 18.52% fivefold coordination, and 33.33% sixfold coordination.

An equilibrium volume for the rapidly quenched glass (Fig. 4) very close to that of the slow cooled glass at 200 K, reflects a more complete relaxation process. This is evident from the 11.1% drop in volume seen during the first 200 time steps of the total 6000 in the rapid quench as opposed to only 8.2% seen for the rapidly quenched glass in case 1.

In order to study any possible crystallization the room temperature glass in case 2 was gradually heated up to 800 K at intervals of 100K, simulations lasting for 1000 time steps at each of the intervals. However, the glass seems to show no obvious signs of any crystallization. The volume tends to

follow the same behavior observed during cooling even on increasing the annealing time to 2000 time steps. The heat treated glass at 800 K shows no change in the average coordination number for the unlike ions from that at 200 K. Experiments carried out by O'Bryan *et al.*[42] on $ZnCl_2$ glass indicate crystallization onset at 470 K. The resistance to crystallization in the computer glass would therefore be due to either the high heating and cooling rates in comparison to the rates observed in laboratory experiments, requiring therefore very long holding times at each of the heat treatment temperatures to perceive any substantial crystallization or the absence of heterogeneous nucleation sites.

V. DISCUSSION

The results of this study have been grouped under three main categories, general principles of glass formation, interatomic potential, and glass formation and the MD technique and glass formation.

A. General principles of glass formation

Results of the simulation of molten NaCl and $ZnCl_2$ at constant pressure show good agreement with generally accepted glass transition rules. Both MX and MX_2 models exhibit discontinuity in the first derivatives of first-order thermodynamic properties (volume, energy, enthalpy) upon cooling. This behavior is characteristic of the glass transition. We have therefore named the temperature at which this discontinuity occurs, the glass transition temperature. In the case of NaCl, the simulation predicts a value for T_g of 2/3 T_m (where T_m is the melting point) which corresponds to the 2/3 rule for conventional ceramic glasses. The lowest calculated T_g for $ZnCl_2$ is 100° above the experimental value. The ratio of the heat capacity of the liquid to the heat capacity of the glass for the model halide systems are well inside the interval of characteristic heat capacity ratios for ionic glasses, i.e., [1.1–1.8]. In the case of NaCl, a ratio of 1.35 was observed whereas a value of 1.2 was estimated for $ZnCl_2$. The temperature dependence of the Gibbs free energy of the different phases involved in the glass formation process can be calculated by traditional thermodynamic expressions if it is written as an integral over the temperature of the differential quantity $dG = dH - d(TS)$ along a reversible path linking the two extreme states. Performing the integration yields

$$G(T) - G(T_0) = H(T) - H(T_0) - T\int_{T_0}^{T} dS.$$

The heat capacity is defined as $C_p = T(dS/dT)_p$. Thus the above expression becomes

$$G(T) = H(T) - T\left[S(T_0) + \int_{T_0}^{T} C_p d\theta/\theta\right].$$

We have applied this expression to the calculation of the Gibbs free energy of the crystalline phase, liquid phase, glassy phase of NaCl. The heat capacities have been taken constant over the interval of temperature of existence of the respective phases and extended to the entire interval (300–1300 K). To overcome the lack of absolute values of free energy we assumed, $G^*_{\text{crystal}(300\,\text{K})} = H_{\text{crystal}(300\,\text{K})}$ as the initiating point for the calculations.

The contrast between the crystal–liquid first-order phase transition and the liquid–glass second-order phase transition is clearly shown in Fig. 7. The liquid is thermodynamically more stable or equally stable than the glass at all temperatures bringing forth the nonequilibrium nature of the glass formation. Similar curves can be obtained for the KDR model for $ZnCl_2$ liquid and glasses for which two T_g values have been reported. The G_{liq} (T) curve constitutes the envelope of all possible G_{glass} (T) curves.

The cooling rates affect the structure of the glass. The change in local structure being evident in the average coordination number for the unlike ions in both the halide systems. Slow cooling rates tend to produce large amounts of the more stable sixfold coordinated cation in the glass. The glass forming ability of the two salts is also reflected in the simulations. The relative ease with which NaCl crystallizes on heating indicates that it is not a good glass former. On the other hand, $ZnCl_2$ shows no signs of crystallization upon heating since heterogeneous nucleation sites are absent in the simulation and only homogeneous nucleation can be observed. The structure of the computer simulated glass is also in good agreement with the available experimental data for $ZnCl_2$ as discussed in Sec. IV.

B. Interatomic potential and glass formation

In the present work, three different effective interatomic potentials have been used. These potentials mimic the behavior of materials with different bonding characteristics. The interatomic potentials for NaCl describe a purely ionic material. The WAC potentials for $ZnCl_2$ give an effective representation of a material with covalent bonds, The KDR potentials reproduce the behavior of a partially covalent system (57% covalent). The large ionicity in two of the models being reflected in the repulsive nature of the potential. The large repulsion term in the potential enhances the hardness of the potential inducing more ionic character. This ionic nature allowing primarily diffusion mechanisms to operate in the relaxation behavior of the glass and the configurational arrest temperature bearing a direct relation to the disappearance of diffusional activity. More pronounced discon-

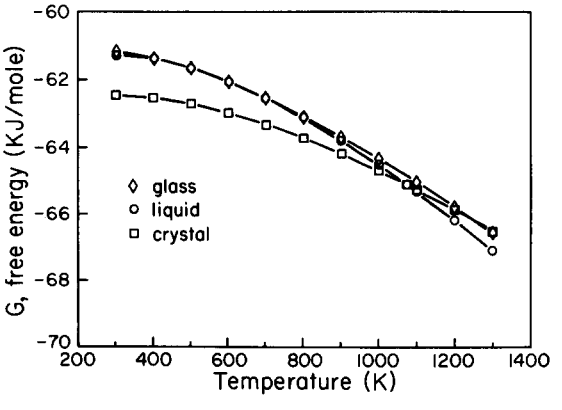

FIG. 7. Calculated free energy vs temperature for glass, liquid, and crystal of NaCl.

tinuities in heat capacity and thermal expansion coefficient are observed for systems with large ionic nature. For the purely ionic systems such as NaCl, the glass transition temperature corresponds to the arrest of any further relaxation and a hard potential leads to large activation energies for diffusional jumps. The increased hardness and ionicity of the potential increases the unlike ion coordination upon cooling towards the more stable octahedral state. The packing of hard spheres dictates the preference of ionic systems for octahedral coordination. However, in the case of the WAC model, the system behaves like a polymeric network. The softness of the potential tends to smear out the glass transition region. This is because the transport properties such as diffusion and viscosity so relevant to glass formation are strongly dependent on the repulsion terms in the pair potential.[43] The polymeric nature of the model allows only steric relaxations and thereby does not alter the structure but only the orientation of the basic polyhedra. As a result, there is no visible glass transition per se in the volume temperature plots, the activation energy for steric relaxation being small.

The KDR model on the other hand induces a combination of network and ionic behavior. Upon cooling there is an increasing trend for the system to accept the preferred sixfold state. However, it may be mentioned that even though on cooling a large fraction of the unlike ions prefer the sixfold state, stoichiometry of the compound limits this transformation to no more than 50%. This increase in the sixfold coordinated cations results in edge sharing polyhedra. The Zn–Zn distance of 4.2 Å for edge sharing octahedra yield a splitting in the cation-cation radial distribution function for the glass [Fig. 5(b)]. This behavior is similar in nature to the splitting of the g_{++} partial radial distribution function for NaCl.

C. MD technique and glass formation

The results discussed in the preceding section show the important role played by the parameter W, the mass of the borders, in the structural relaxation and the ionic mobility in the glass. A large value for this parameter lowers the mobility of the ions, in effect, increasing the viscosity and bringing about an early arrest in the structure. The glass transition temperature T_g scales with W. It may be noted that a very large value for W would make the borders totally rigid simulating conditions of constant volume which is not a satisfactory procedure to simulate a normal laboratory condition for obtaining glasses. On the other hand, lowering the value for the parameter W increases the diffusion rate of the ions which in turn allows more ions to occupy the preferred sixfold coordinated state. As shown in Sec. IV at low temperatures a larger fraction (8.3%) of the cations favor octahedral sites in the glass for the system with a not so rigid boundary wall (i.e., $W = 5$) in comparison to the glass with a more rigid boundary ($W = 50$). In as much as the coordination of the ions are affected the mass of the borders seem to have a negligible effect on the radial distribution function. A close similarity can be drawn in the results obtained with the mass of the borders and the cooling rate. Lowering the mass appropriately correlates to a slower cooling rate and consequently a lower glass transition. One can therefore envisage that a further decrease in the value of W could be advantageous in lowering the glass transition further beyond 500 K of the $ZnCl_2$ system. However, long computational times needed for obtaining good equilibrium values and the computational costs involved would make this operation an uphill task.

CONCLUSIONS

This paper highlights the use of MD in studying the structure and glass formation of simple ionic systems such as NaCl and $ZnCl_2$, the former being an example of MX salt and the latter of MX_2 systems. In conclusion it can be summarized that the technique of molecular dynamics within the use of proper scientific jurisdiction provides valuable structural and thermodynamic information. The technique is mainly governed by the accuracy of the interatomic potential. In all cases the technique provides results that are in agreement either with experiment wherever available or with the general rules for glass formation. The present study has been mainly directed towards the study of the structure of the liquid and glass formation. Future work will be focussed on the potential of the technique for obtaining information on optical properties such as the infrared transmission.

ACKNOWLEDGMENTS

The authors are very grateful to the Center for Computing and Information Technology and the College of Engineering and Mines at the University of Arizona for generous allocations of computing time.

[1]D. Frenkel and J. P. McTague, Annu. Rev. Phys. Chem. **31**, 491 (1980).
[2]L. V. Woodcock, in *Structure and Mobility in Molecular and Atomic Glasses*, edited by J. M. O'Reilly and M. Goldstein (Annals of the N.Y. Acad. of Sciences, New York, 1981).
[3]C. A. Angell, J. H. R. Clarke, and L. V. Woodcock, Adv. Chem. Phys. **48**, 397 (1981).
[4]A. Rahman, R. H. Fowler and A. H. Narten, J. Chem. Phys. **57**,3010 (1972).
[5]T. F. Soules, J. Chem. Phys. **71**, 4570 (1979).
[6]L. V. Woodcock, C. A. Angell and P. Cheeseman, J. Chem. Phys. **65**, 1565 (1976).
[7]J. Lucas, C. A. Angell, and S. Tamaddon, Mater. Res. Bull. **19**, 945 (1984).
[8]C. C. Phifert and C. A. Angell, Bull. Am. Ceram. Soc. **65**, 533 (1986).
[9]Y. Kawamoto, T. Horisaka, K. Hirao, and N. Soga, J. Chem. Phys. **83**, 2398 (1985).
[10]L. T. Hamill and J. M. Parker, Mat. Sci. Forum **6**, 437 (1985).
[11]I. Yasui and H. Inoue, J. Non-Cryst. Solids **71**, 39 (1985).
[12]S. A. Brawer and H. J. Weber, J. Chem. Phys. **75**, 3522 (1981).
[13]J. H. Simmons, R. Faith, and G. O'Rear, Mat. Sci. Forum **19–20**, 121 (1987).
[14]E. J. W. Verwey, Recl. Trav. Chim. Pays-Bas, Belg. **65**, 521 (1946).
[15]J. H. R. Clark, J. Chem. Soc. Faraday Trans. 2 **75**, 1371 (1979).
[16]C. S. Hsu and A. Rahman. J. Chem. Phys. **71**, 4974 (1979).
[17]M. Amini and R. W. Hockney, J. Non-Cryst. Solids **31**, 447 (1979).
[18]J. A. Erwin Desa, A. C. Wright, J. Wong, and R. N. Sinclair, J. Non-cryst. Solids **51,57** (1982).
[19]P. J. Gardner and D. M. Heyes, Physica **131B**, 227 (1985).
[20]S. Inoue, M. Tamaki, H. Kawazoe, and M. Yamane, J. Mater. Res. **2**, 357 (1987).
[21]K. Hirao and N. Soga, J. Non-Cryst. Solids **95–96**, 577 (1987).
[22]S. Biggin and J. E. Enderby, J. Phys. C **14**, 3129 (1981).

[23]P Ballone, G. Pastore, J. S. Thakur, and M. P. Tosi, Physica **142B**, 294 (1986).
[24]P. N. Kumta, P. A. Deymier, and S. H. Risbud, Physica **153B**, 85 (1988).
[25]M. Parrinello and A. Rahman, J. Appl. Phys. **52**, 7182 (1981).
[26]A. Rahman and M. Parrinello, in *The Physics of Superionic Conductors and Electrode Materials*, NATOASI, odense, edited by J. Perran (Plenum, New York, 1980).
[27]M. Parrinello, A. Rahman, and P. Vashista, Phys. Rev. Lett. **50**, 1073 (1983).
[28]P. P. Ewald, Ann. Phys. (Paris) **21**, 1087 (1921).
[29]G. S. Crest and S. R. Nagel, J. Chem. Phys. **91**, 4917 (1987).
[30]H. C. Andersen, J. Chem. Phys. **72**, 2384 (1980).
[31]L. V. Woodcock, Chem. Phys. Lett. **10**, 257 (1971).
[32]S. Nose, J. Chem. Phys. **81**, 511 (1984).
[33]S. Nose, Mol. Phys. **57**, 187 (1986).
[34]M. J. L. Sangster and R. M. Atwood, J. Phys. C **111**, 1541 (1978).
[35]C. A. Angell and J. C. Tucker, J. Phys. Chem. **78**, 278 (1974).
[36]J. H. Hildebrand, Science **174**, 490 (1971).
[37]F. G. Edwards, J. E. Enderby, R. A. Howe, and D. I. Page, J. Phys. C **8**, 3483 (1975).
[38]M. J. L. Sangster and M. Dixon, Adv. Phys. **25**, 247 (1976).
[39]G. S. Cargill, Solid State Phys. **30**, 227 (1975).
[40]M. R. Hoare, J. Non-Cryst. Solids **31**, 227 (1975).
[41]S. Nose and F. Yonezawa, J. Chem. Phys. **84**, 1803 (1986).
[42]H. M. O'Bryan, Jr., L. G. Van Uitert, H. J. Guggenheim, and W. H. Grodkiewicz, Bull. Am. Ceram. Soc. **58**, 1098 (1979).
[43]C. A. Angell, J. H. R. Clarke, and L. V. Woodcock, Adv. Chem. Phys. **48**, 397 (1981).